Materials Reports Solidwaste & Ecomaterials

Materials Reports: Solidwaste and Ecomaterials

Journal Homepage: www.sciopen.com/journal/3078-4093

Original Research Report

Purifying marine clay for the preparation of LC^3

Qi Luo [1, 2], Xinyu Zhang [2], Yin Bai [2], Guoqing Geng [1, *]

[1] Department of Civil and Environmental Engineering, National University of Singapore, 117576, Singapore

[2] Department of Civil Engineering, Chongqing Jiaotong University, Chongqing, 400074, China

Abstract: Recent studies suggest that marine clay has the potential to substitute cement after calcination, although its reactivity is limited. This paper evaluates the purification of Singapore marine clay, which mainly consists of low kaolinite and high quartz, for use as a cement substitute. The study explores wet sedimentation and surfactant-assisted sedimentation to enhance reactivity in a typical limestone calcined clay cement (LC^3) recipe by reducing quartz content. The findings indicate that while wet sedimentation effectively removes quartz, it is less effective for silt due to its smaller size. Surfactant-assisted sedimentation further purifies the clay, with material strength depending on both composition and particle size. Specifically, clay filtered through a 22 μm sieve exhibited improved strength. The study recommends the 22-WS-CC method for its cost-efficiency and feasibility in large-scale implementation without chemical reagents. Overall, this research contributes to the sustainable development of the construction industry by providing insights into the effective utilization of low-grade, impure clays in cement production.

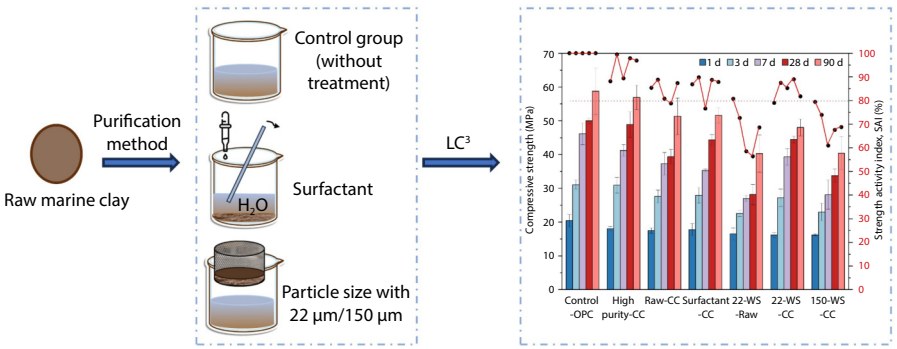

Keywords: marine clay, limestone calcined clay cement, kaolinite, sedimentation, hydration, strength

Citation: Q. Luo, X. Zhang, Y. Bai, G. Geng. Purifying marine clay for the preparation of LC^3. *Materials Reports: Solidwaste and Ecomaterials*, 2025, 1: 9520008. https://doi.org/10.26599/MRSE.2025.9520008.

1. Introduction

Replacing ordinary Portland cement (OPC) with alternative materials is currently the most viable approach towards achieving low-carbon concrete production[1-3]. Among these alternatives, limestone calcined clay cement (LC^3) has recently emerged as an environmentally friendly option[4]. LC^3 is composed of a blend of limestone and calcined clay, allowing for a reduction in clinker content by up to 50%[4-7], thereby significantly reducing energy consumption compared to OPC. Moreover, establishing production plants near large clay deposits can lead to a 40% reduction in CO_2 emissions, a 33% decrease in costs, and a 22% reduction in embodied energy, thus promoting cleaner and more sustainable cement production[8,9]. Despite these reductions, LC^3 maintains mechanical strength and durability equivalent to that of OPC[10-13]. The growing interest in LC^3 technology highlights its economic appeal and potential to drive sustainable development within the cement industry[14-19].

Clays, primarily alumino-silicates, generally exhibit stability under neutral and alkaline conditions. Calcined clays are produced through thermal treatment of clays at temperatures ranging from 600 °C to 900 °C[12,20], a process that causes the mineral kaolinite within the clay to lose its bound hydroxyl groups, enhancing its reactivity in alkaline environments. When the kaolinite within clay is calcined, it trans-

*Correspondence to G. Geng, ceegg@nus.edu.sg

Received 16 September 2024; Received in revised form 16 January 2025; Accepted 5 March 2025

forms into metakaolin, a product known for its reactivity. Therefore, clays with higher kaolinite content produce a greater amount of reactive components after calcination[21]. Although metakaolin does not independently react with water, it undergoes hydration in the alkaline environment of cement paste, generating new hydration products that integrate into the cement microstructure.

Research has shown that the calcined kaolinite content is crucial in determining the strength of LC^3 [11,13,22,23]. However, most kaolinite deposits worldwide consist of mixed clays, where kaolinite is accompanied by other minerals such as quartz, carbonates, and metal oxides[9]. Recent studies have demonstrated that even impure clays can be calcined to produce satisfactory LC^3, provided the clay contains at least 40% kaolinite by mass[12,24-28]. Utilizing these impure clays, often considered an environmental burden, can lead to even significant cost savings compared to high-grade clays. To further expand the use of clay deposits, separation techniques such as sedimentation can be employed to segregate kaolinite from other minerals like quartz, especially when the kaolinite content is low[29,30]. This approach enables the conversion of low-purity clays into viable supplementary cementitious materials (SCMs) or the production of more reactive SCMs from marginal clays. Sedimentation, a commonly used method, separates associated minerals based on particle size disparities, while chemical treatments (including surfactant-assisted methods), can further enhance impurity removal.

The application of this concept to marine clays, which are abundant in coastal areas, presents an intriguing avenue for further investigation. Marine clays, typically low-grade kaolinite clays, are composed of marine sediments and are widely distributed in coastal regions around the world[31-34]. Unlike regular clay, marine clay exhibits higher initial water content due to its coastal environment. In Singapore, for example, marine clay primarily consists of quartz and kaolinite, with secondary minerals such as mica and smectite[35]. A significant portion of this clay is excavated from tunnels, foundations, and other construction sites, posing challenges for waste management and disposal. Marine clay is one of the predominant geological materials covering downtown and the central business district of Singapore[36]. Large quantities are excavated annually, particularly during underground rail system construction[37]. Despite its prevalence, marine clay is currently treated as waste. However, its potential uses, including brick making[38] and hazardous waste stabilization[39], have been explored. The disposal of marine clay in landfills is prohibited by legislation in Singapore, underscoring the critical need for alternative uses[40].

This study aims to evaluate and compare the effectiveness of two purification methods—wet sedimentation and surfactant-assisted sedimentation—on marine clay, which consists of approximately 20% kaolinite, 35% quartz, 25% illite, and various other amorphous substances[41]. Additionally, the pozzolanic reactivity and properties of LC^3 incorporating these purified calcined clays were investigated to validate their potential application. This research is expected to pave the way for the utilization of marine clay in construction, particularly in Singapore and other coastal areas, thereby transforming a previously underutilized resource into a valuable component of sustainable building materials.

2. Materials and methods

2.1. Raw materials

The clay material used in this study was sourced from a construction site project near Changi Airport in Singapore, as depicted in Fig. 1. Initially, the raw clay was dried at 85 °C for 72 h, after which it underwent two purification processes:

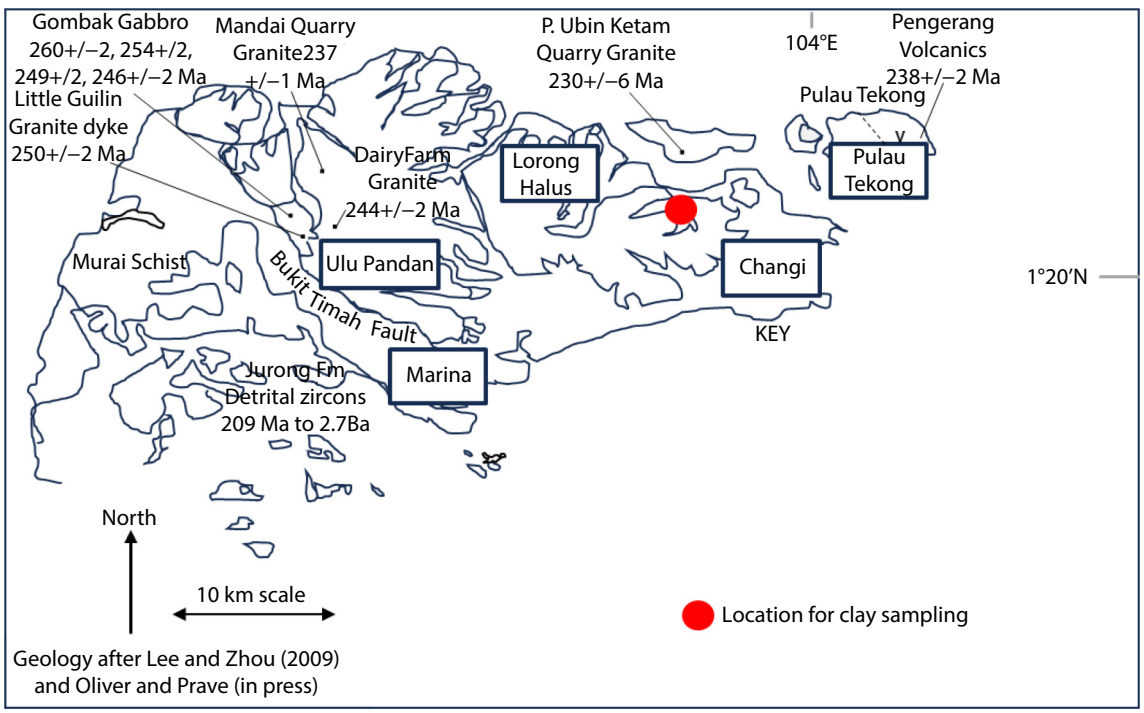

Fig. 1. Geological map of Singapore with location for clay sampling. Reproduced with permission from Ref. [42].

wet sedimentation and surfactant-assisted sedimentation. The following steps outline the preparation procedure for the waste marine clay:

1) Crushing raw clay: The raw clay was first crushed into smaller particles using a crusher.

2) Suspension in water or dispersant solution: The crushed particles were then suspended in either water or a dispersant solution, ensuring thorough dilution of the raw clay.

3) Wet sedimentation process: The diluted clay suspension was sieved through mesh sizes of either 22 μm or 150 μm, and the liquid that passed through these sieves was collected.

4) Drying of sedimented liquid: The collected liquid was subsequently dried at 40 °C over 5–7 d.

5) Ball milling: Once dried, the clay was subjected to ball milling for 30 min to achieve finer particle sizes, which were measured using a laser diffraction particle size analyzer (Bettersize 2600), as shown in Table 1.

6) Calcination: Finally, the processed clay was calcined by heating to 800 °C and maintaining this temperature for 1 h, as suggested by Ref. [12].

This procedure resulted in two distinct samples before calcination—22-WS-Raw (sieved with 22 μm mesh) and 150-WS-Raw (sieved with 150 μm mesh)—and two samples after calcination (22-WS-CC and 150-WS-CC). The same steps were followed for samples prepared using the dispersant method, as illustrated in the simplified flowchart of the clay treatment process (Fig. 2).

For the surfactant preparation[30], 50 g (approximately 20 mL) of dried raw clay was vigorously mixed with 125 mL of deflocculating solution at various concentrations using a high-shear mixer for 2 min. The resulting slurry was transferred to graduated cylinders and topped up with distilled water to 1000 mL. The cylinders were then inverted multiple times to ensure homogeneity. During a 24-hour settling period, quartz particles settled out while the clays remained in suspension. After this period, the remaining suspension was extracted, dried, milled, and finally calcined to produce the surfactant calcined clay, referred to as Surfactant-CC. Additionally, a control group of high-purity calcined clay (High purity-CC) was prepared, featuring an initial kaolinite content of over 97%. The chemical compositions of the various clays were analyzed using X-ray fluorescence spectroscopy (PANalytical Zetium, Netherlands), with detailed results presented in Table 2. The transformation of the raw clay material into processed clay can be seen in Fig. 3, where calcination changes the color from gray to reddish-brown.

Compressive strength tests (ASTM C311[43]) were conducted with mixes containing CEM I 52.5 N OPC, and the results were used as an indirect measure of the pozzolanic activity of clay.

2.2. Sample preparation

The powders were first mixed for 1 h using a core mixer to

Table 1. Particle size of marine clay (μm).

Particle size	Raw-clay	Raw-CC	Surfactant-CC	22-WS-Raw	22-WS-CC	150-WS-CC	High purity-CC
Dv10	1.605	1.488	2.687	1.523	2.396	2.403	3.446
Dv50	7.038	9.491	25.33	4.806	16.78	16.62	9.237
Dv90	28.73	43.87	590	16.98	58.41	55.03	19.62

Note: Surfactant-CC is hand-milled (due to the small quantity), resulting in a Dv90 particle size of 590 μm.

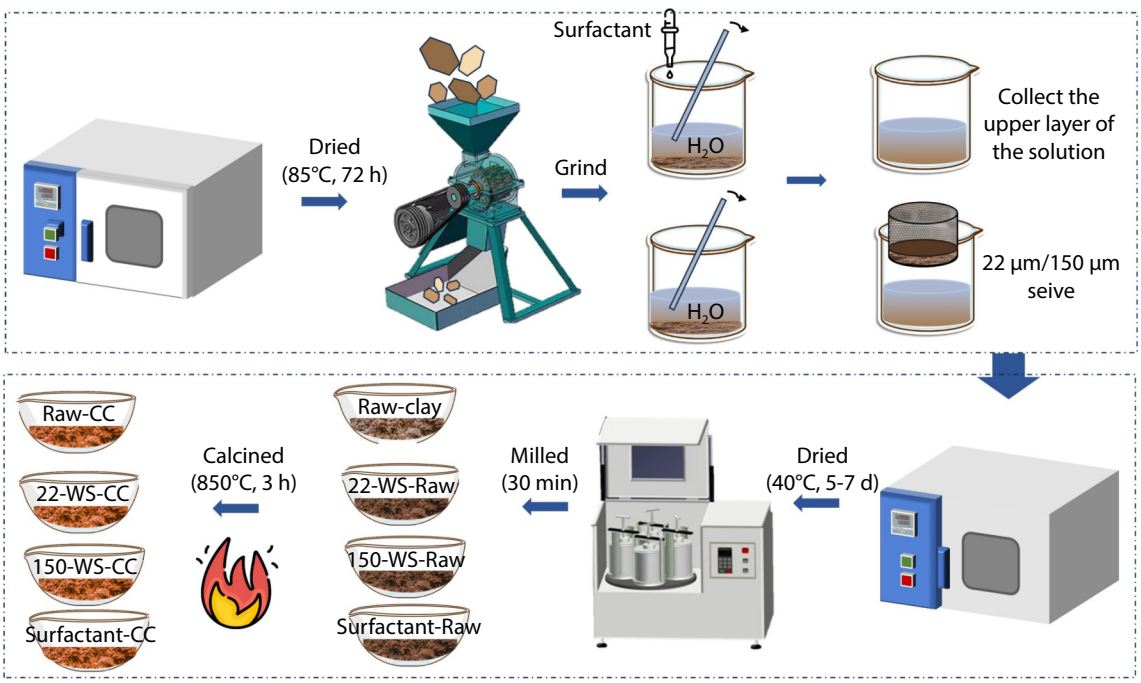

Fig. 2. Flowchart of the clay treatment process.

Table 2. Chemical analysis for marine clay, cement, limestone, and gypsum (wt%).

Chemical composition	Raw-clay	Raw-CC	Surfactant-CC	22-WS-Raw	22-WS-CC	High purity-CC	Cement	Limestone	Gypsum
Na_2O	1.09	1.05	2.18	1.11	1.20	-	0.24	0.07	0.11
MgO	1.73	1.51	1.93	1.73	1.79	-	3.58	0.68	0.53
Al_2O_3	21.41	21.58	25.04	24.84	25.55	44.23	4.40	0.87	0.32
SiO_2	64.25	66.69	58.93	61.41	60.79	54.31	20.31	1.25	0.43
SO_3	0.95	1.02	0.87	0.80	1.29	-	3.68	0.03	56.49
K_2O	2.07	1.86	2.43	2.16	2.26	-	0.89	0.09	0.02
CaO	2.65	1.34	1.25	1.57	1.55	-	62.58	96.44	39.50
Fe_2O_3	4.28	3.89	5.47	4.45	4.40	-	3.7	0.44	0.11
Others	1.57	1.06	1.9	1.93	1.17	1.46	0.62	0.13	2.49

Fig. 3. Pictures of (a) Raw-clay, (b) 22-WS-Raw, (c) Raw-CC, (d) 22-WS-CC, (e)150-WS-CC, (f) Surfactant-CC, (g) High purity-CC.

achieve uniform color. Sand was then introduced and mixed for 3 min. Subsequently, the liquid was added, and the mixture was further blended for an additional 4 min. The fresh mortar was then cast into 40 mm × 40 mm × 40 mm cubic molds, following the guidelines specified in EN 196-1-2016[44]. The mix design used a binder:sand:water ratio of 1:3:0.5, with the binder containing calcined clay, cement, limestone, and gypsum. The samples were cured in water at a controlled temperature of 20±2 °C. Specific mix proportions are detailed in Table 3.

Calorimetric measurements were performed using the Thermometric TAM Air system, monitoring hydration of 10 g fresh paste samples at 20 °C for 3 d. Additionally, X-ray diffraction (XRD) was employed to investigate the hydration process. Cement paste samples were prepared with a water-to-binder ratio of 0.5 and stored in 15 mL sealed plastic vials at 20 °C. The hydration process was halted after 7 d using isopropanol, followed by drying in an oven at 40 °C for 48 h.

The modified R^3 test[45] was conducted to assess the pozzolanic reactivity in a simulated calcium-rich alkaline environment. In this test, analytical reagent CH powder was combined with the SCMs at a mass ratio of 3:1. The powders were manually mixed for 4 min to achieve homogeneity. Subsequently, 0.5 M potassium hydroxide (KOH) solution was introduced, producing a homogeneous paste with a liquid-to-solid ratio of 0.9. The paste was further mixed manually for 4 min in a beaker.

For each material, 38.0 g of modified R^3 paste was pre-

Table 3. Mix designs for cement, calcined clay, limestone, and gypsum (wt%).

Mixture	Cement	Calcined clay	Limestone	Gypsum
Control-OPC	100	-	-	-
High purity-CC	80.12	13.11	6.37	0.40
Raw-clay	80.12	13.11	6.37	0.40
Raw-CC	80.12	13.11	6.37	0.40
Surfactant-CC	80.12	13.11	6.37	0.40
22-WS-Raw	80.12	13.11	6.37	0.40
150-WS-Raw	80.12	13.11	6.37	0.40
22-WS-CC	80.12	13.11	6.37	0.40
150-WS-CC	80.12	13.11	6.37	0.40

pared, comprising 5.0 g of SCM, 15.0 g of $Ca(OH)_2$, and 18.0 g of KOH solution. To minimize evaporation and carbonation, the paste was sealed in plastic vials and cured in a 50±2 °C oven until the designated testing age. Separate containers were used for each testing age, with two testing ages (1 d and 7 d) being evaluated.

2.3. Testing program

2.3.1. X-ray diffraction (XRD)

XRD was employed to identify the crystalline minerals in the untreated soil and observe the mineralogical changes post-treatment. The XRD analysis was conducted using an Ultima IV diffractometer, where raw and processed clays were blended with CaF_2 at a weight ratio of 1:4 (CaF_2: paste). The analysis was performed with Cu-Kα radiation operating at 40 kV and 40 mA. The scanning range was set from 5° to 60° (2θ), with a scanning step size of 0.02° and a scanning speed of 0.25 s/step. It should be noted that quantitative measurements can be affected by amorphous factors, limiting precision. Therefore, XRD was primarily used to observe approximate trends across different system phases, while thermogravimetric analysis (TGA) provided quantitative measurements of $Ca(OH)_2$ to assess hydration products.

2.3.2. Isothermal calorimetry

To examine the initial hydration process, isothermal calorimetry was performed on 3-day samples at 20 °C using a TAM Air system (TA Instruments). The paste, formulated with a water-to-binder (w/b) ratio of 0.5, was mixed using an electric stirrer at 1200 rpm for 2 min. Subsequently, 10 g of the paste was transferred into an ampoule and placed within the calorimeter.

2.3.3. Bound water and calcium hydroxide consumption

TGA was employed as a reference technique to determine the amount of bound water and calcium hydroxide consumed[46]. After curing for 3 d and 7 d, 30–40 mg of material was extracted from the paste center and placed into a pre-weighed ceramic crucible. The paste was analyzed without hydration stoppage from room temperature to 600 °C at a heating rate of 10 °C min^{-1}. The test was performed under a nitrogen (N_2) atmosphere with a constant flow rate of 20 mL min^{-1}.

2.3.4. Mercury intrusion porosimetry (MIP)

Mortar specimens, hydrated for 28 d, were cut into small test pieces less than 1×1×1 cm^3. The MIP test was conducted using an Autopore V 9620 instrument with mercury intrusion pressure up to 60000 psi. The surface tension of mercury was measured at 0.485 N m^{-1}, with a contact angle of 130°.

2.3.5. Compressive strength

Compressive strength testing was conducted at 1, 3, 7, 28, 90 d, with a loading rate of 2.4 kN s^{-1}. The compressive strength of the mortar was determined by testing three samples at each specified age[46].

3. Results and discussion

3.1. X-ray diffraction analysis

The XRD results for both raw and treated clays are presented in Fig. 4. The analysis identifies illite, kaolinite, and quartz as the primary clay minerals in the uncalcined marine clay, consistent with previous studies on Singapore marine clay[47,48]. After surfactant treatment or sieving (Figs. 4b, 4c), a reduction in quartz content is observed in the raw clay, while the proportions of illite and kaolinite increase. This increase in kaolinite content suggests an impact on the overall composition of the clay matrix. The reduced intensity of the XRD patterns can be attributed to the diminished presence of quartz in the treated samples. Upon calcination, the kaolinite transforms and disappears, indicating a conversion from crystalline kaolinite to an amorphous state. Despite these changes, the XRD patterns of both untreated and treated marine clay samples exhibit similarities (Fig. 4a), with no observable new mineral formations, suggesting that the treatment process did not induce the creation of any new minerals.

The thermogravimetry analysis (TGA) and derivative thermogravimetry (DTG) curves (Fig. 5) display the removal of OH groups within the 350–650 °C, characteristic of kaolinite[49,50]. As noted by Du et al.[49], the location of the dehydroxylation peak depends on the structure type and the bonding of hydroxyl groups. Additionally, the shape and range of the XRD peak are sensitive to factors such as crystallinity and particle size distribution[51]. For the marine clay sample, the presence and amount of kaolinite can be directly correlated with water loss during the dehydroxylation process (400–650 °C), allowing for the estimation of kaolinite content in the marine clay. Graphical analysis indicates that the treated clay exhibits a higher kaolinite content compared to the raw clay, consistent with the XRD findings. This suggests that the treatment process has increased the concentration of kaolinite in the clay sample, influencing its overall composition.

3.2. Hydration heat evolution

The early hydration behavior of the mixtures was investigated using isothermal calorimetry. Fig. 6 presents the heat evolution curves over 72 h for different pastes. Comparing Control-OPC to the paste with 20% cement replaced by clay and limestone reveals minimal deviation in the onset time and reaction rate. The graph shows that within the first 12 h, the peak of the silica hydration reaction in OPC is the highest. In the LC^3-80 system, although the peak value of the silica hydration reaction decreases, it occurs earlier, likely due to the filler effect promoting cement hydration[52]. Minor variations in the timing of the silica hydration peak can be attributed to differences in clay particles. The mixture with 20% calcined clay and limestone replacing cement shows weaker reactivity than OPC but higher pozzolanic reactivity than the original marine clay after undergoing various treatments.

The mixture with added clay also displays a distinct heat release peak (~10 h), indicating the C_3A reaction[53]. This can be linked to the high aluminum content in the clay, which interacts with the CH environment after cement hydration, promoting the C_3A reaction. Between 24–30 h, a peak corresponding to the aluminate hydration reaction is observed[54]. The timing of the aluminum reaction peaks is consistent across samples. Among them, the calcined clay treated with a 22 μm sieve shows the lowest reaction peak, while the clay treated

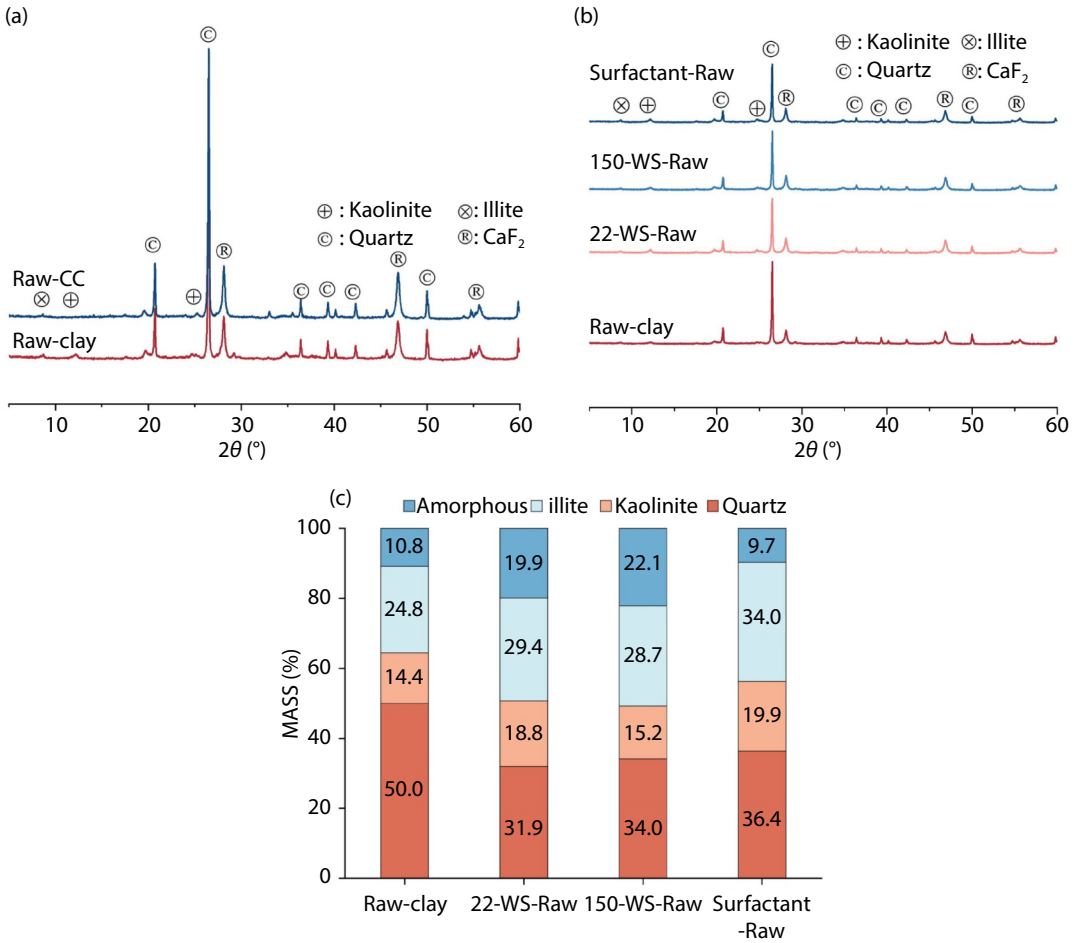

Fig. 4. XRD patterns of marine clay (a) before and after calcination, (b) before and after purification treatment, and (c) quantitative analysis of the XRD results.

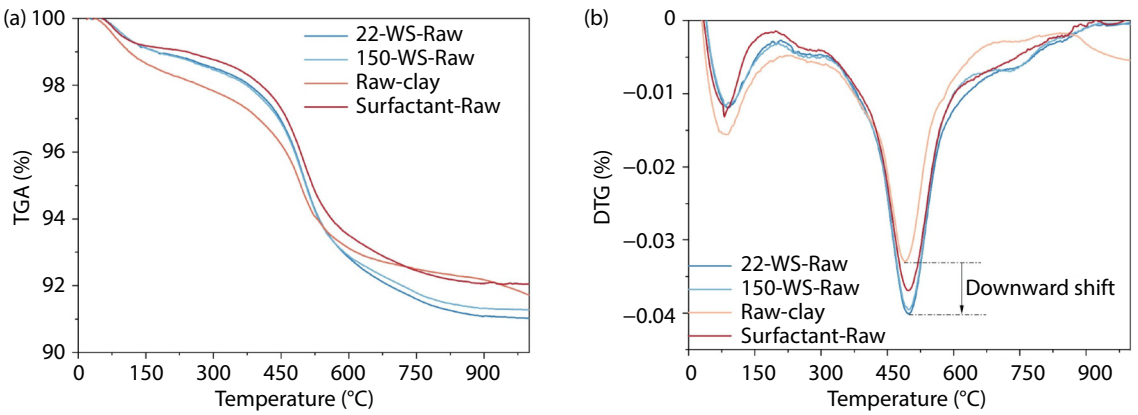

Fig. 5. (a) TGA and (b) DTG curves of marine clay.

with a 150 μm sieve demonstrates a higher degree of reaction, surpassing that of the Surfactant-CC and High purity-CC samples.

3.3. Modified R³ test

The XRD patterns of mixtures prepared using the modified R³ method at 3 d and 7 d are shown in Fig. 7. The various treatment methods had minimal impact on these XRD patterns. Analysis of the reference sample, 22-WS-Raw, revealed a distinct peak corresponding to free CH. In contrast, mixtures containing calcined marine clay exhibited a reduced CH diffraction peak intensity, particularly in the High purity-CC sample. This reduction in CH intensity can be attributed to the pozzolanic reaction of the reactive phases in the calcined clay, which react with CH released during cement hydration, effectively consuming it. Consequently, the CH peak intensity diminishes in the XRD patterns of mixtures containing calcined clay, indicating that calcined clay enhances the overall cementitious properties by efficiently utilizing CH.

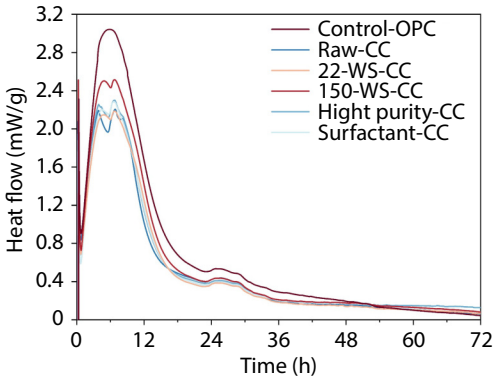

Fig. 6. Heat release during paste hydration.

Fig. 7b demonstrates that pozzolanic reactivity can be further enhanced through additional processes such as sieving and surfactant use. Among the two sieved mixtures, 22-WS-CC exhibited higher CH consumption compared to 150-WS-CC, indicating that finer particle sizes obtained through the 22 μm sieve contributed to a more effective pozzolanic reaction, resulting in greater CH content reduction. Additionally, the high-purity calcined clay showed the highest pozzolanic reactivity among the tested mixtures, as evidenced by the lowest CH content percentages at 3 d and 7 d (22.2% and 16%, respectively). These findings indicate that high-purity calcined clay underwent a significant pozzolanic reaction, leading to substantial CH consumption over time. The enhanced pozzolanic reactivity achieved through sieving and surfactant utilization, combined with the superior performance of high-purity calcined clay, highlights the potential for optimizing the use of clay-based materials in cementitious systems. By leveraging the pozzolanic properties of these materials, it is possible to reduce reliance on cement and enhance the sustainability of construction practices.

Fig. 8 presents the thermogravimetric curves for 3 d and 7 d, showing weight loss in marine clay samples as a function of temperature. The major weight loss at 400–500 °C is associated with the removal of OH groups[55]. Temperature li-

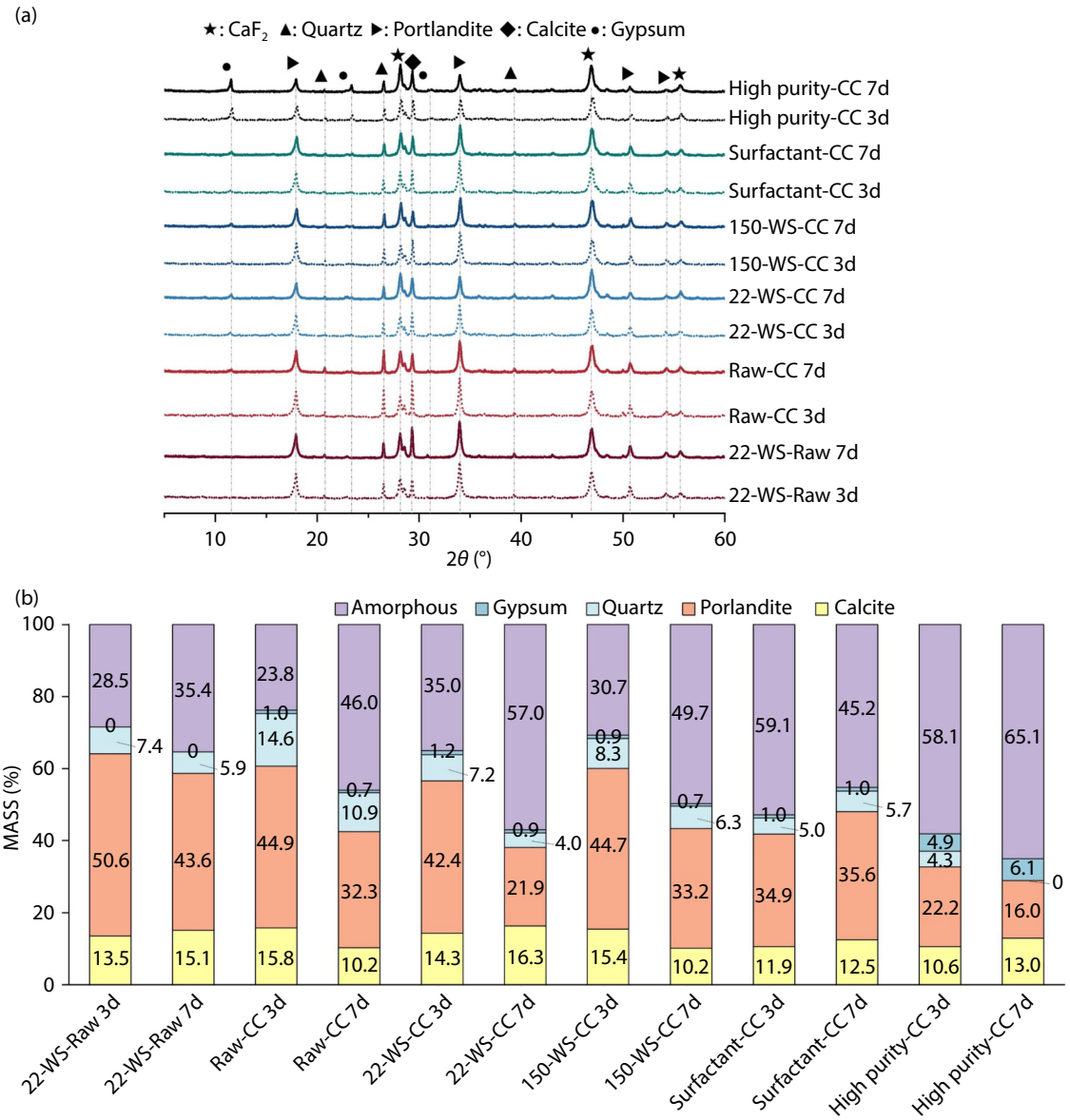

Fig. 7. XRD results following the R³ test: (a) diffraction pattern and (b) quantification.

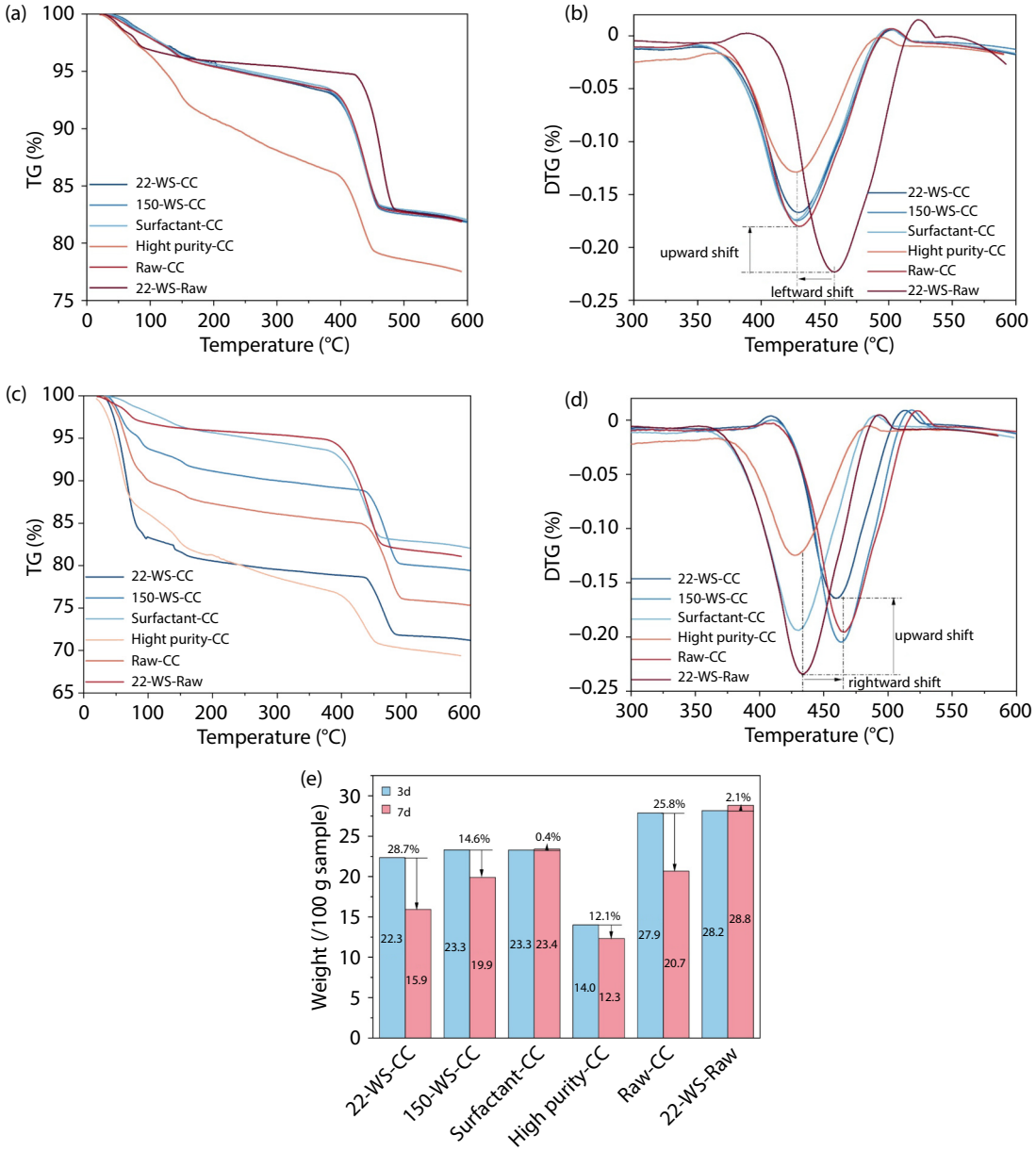

Fig. 8. TGA and DTG of hydrated paste at (a, b) 3 d and (c, d) 7 d, (e) Quantitative analysis of CH.

mits were determined using DTG[56], and the phases were quantified using the tangent method on TGA curves[57]. The XRD results show that the paste containing raw marine clay exhibits the highest CH content. This is likely because active components in the clay, after calcination, consume the CH initially present in the system. Throughout the testing period, High purity-CC consistently exhibits the lowest CH content, indicating superior pozzolanic reactivity. Meanwhile, CH content in paste systems incorporating calcined clay after various treatments remains at intermediate levels, suggesting that the employed treatment methods moderately impact the pozzolanic reaction and CH consumption. Despite the reduced CH diffraction peak intensity, the overall CH content in these paste systems does not match the low levels observed in high-purity calcined clay.

Quantitative analysis of CH in Fig. 8e reveals that 22-WS-CC exhibits the greatest change in CH content between 3 d and 7 d (28.7%), indicating significant enhancement in pozzolanic reactivity during this period. Additionally, 22-WS-CC shows the lowest CH content at 7 d (15.9%), apart from High purity-CC. Conversely, 22-WS-Raw consistently shows the highest CH content at both 3 d and 7 d (28.2% and 28.8%, respectively), suggesting that the calcination process effectively enhances the pozzolanic activity of marine clay. Notably, an increase in CH content from 3 d to 7 d (as observed in Surfactant-CC and 22-WS-Raw) may result in lower compressive strength.

3.4. MIP analysis

The impact of dispersants and the use of a 22 μm sieve on the pore distribution of marine clay and OPC mortar is illustrated in Fig. 9. Initially, upon replacing OPC with marine clay, the porosity of the samples increases, predominantly in the form of thin mesopores (Fig. 9c). The introduction of marine clay introduces additional void spaces within the cementi-

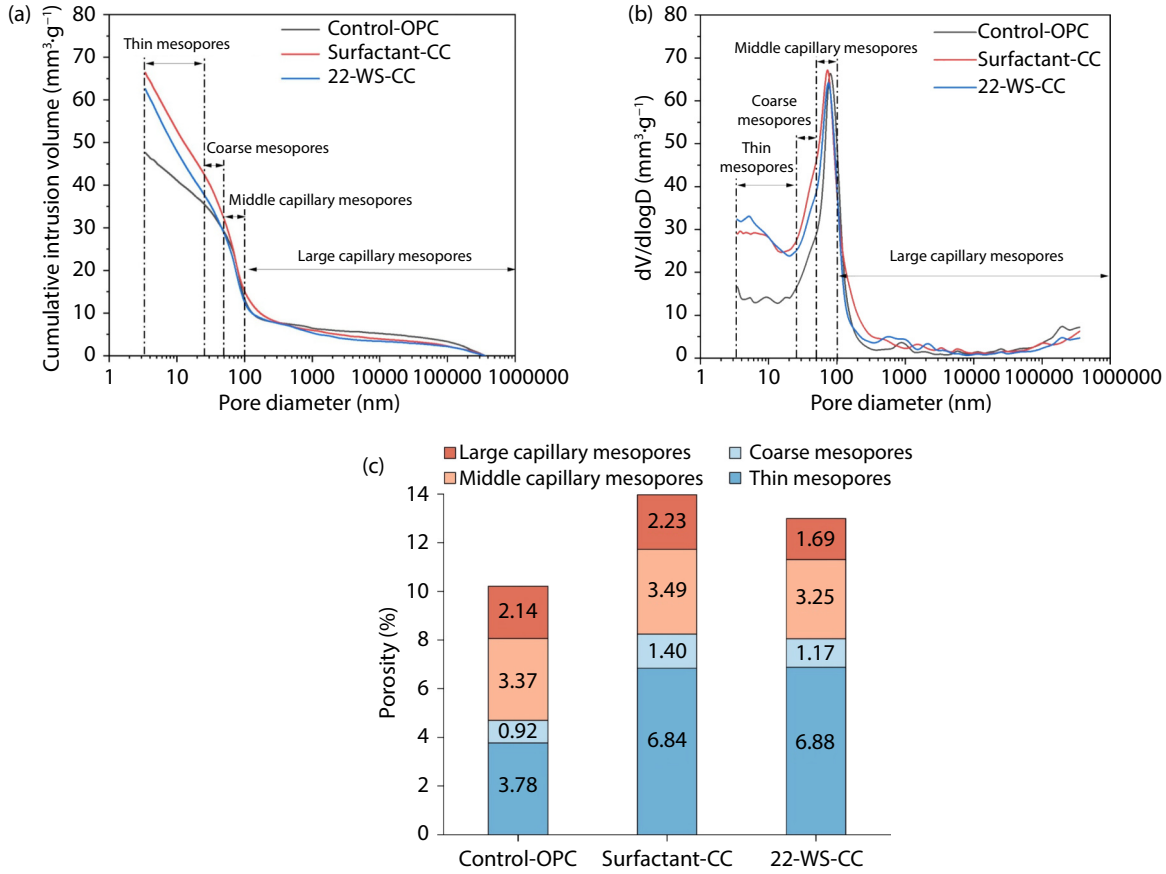

Fig. 9. Porosity by mercury intrusion in mortars at 28 d.

tious matrix, resulting in an overall increase in porosity. These thin mesopores enhance the interconnectedness of the pore network, potentially improving the transport of fluids and gases within the material[3].

In contrast, samples treated with a surfactant and filtered through a 22 μm sieve exhibit similar proportions of different pore sizes compared to untreated samples. The surfactant treatment and sieving process refine the particle size distribution and enhance sample homogeneity, resulting in a more uniform distribution of pore sizes. However, it is important to note that samples passing through the 22 μm sieve show a reduction in the number of middle capillary mesopores and large capillaries compared to untreated samples. Generally, pore volumes in the 100–1000 nm range adversely affect the strength of cementitious materials[3]. This indicates that the sieving process effectively removes larger particles and aggregates, thereby reducing the volume of larger capillary pores and middle capillary mesopores. This sieving process contributes to a finer pore structure, potentially enhancing the mechanical properties and durability of the cementitious material.

3.5. Compressive strength

Fig. 10 illustrates the progression of compressive strength in various mortar mixes. The control OPC consistently demonstrates the highest compressive strength, achieving 49.98 MPa at 28 d of testing. In contrast, the mortar containing 22-WS-Raw exhibits the lowest strength at all testing ages. This is attributed to the non-calcined clay lacking reactive substances, with strength primarily dependent on cement hydration. On the other hand, the calcination process enhances the clay's reactivity, facilitating the reaction with CH to form C-(A)-S-H, which improves strength[58]. This difference underscores the enhanced activation of clay components due to calcination, leading to the formation of more durable cementitious products.

These findings indicate that the internal active components of marine clay can be enhanced through the calcination process, thereby improving the compressive strength of its mixture. Furthermore, the strength of marine clay-based mortar can be further increased through sieving and surfactant treatment. The optimization of the calcination process, sieving techniques, and surfactant treatments can elevate the strength and improve the performance of cementitious mixtures incorporating marine clay as a supplementary cementitious material. The treated marine clays (22-WS-CC, Surfactant-CC, Raw-CC) achieved 80% of the OPC strength at most curing ages, demonstrating the effectiveness of these treatment methods. Particularly, 22-WS-CC with marine clay as the raw material showed good compressive strength at all curing ages, indicating that this treatment method effectively enhances the pozzolanic activity of marine clay, providing significant guidance for future research.

4. Conclusion

This study examines the properties of marine clay treated with various methods to reduce the content of quartz, as well

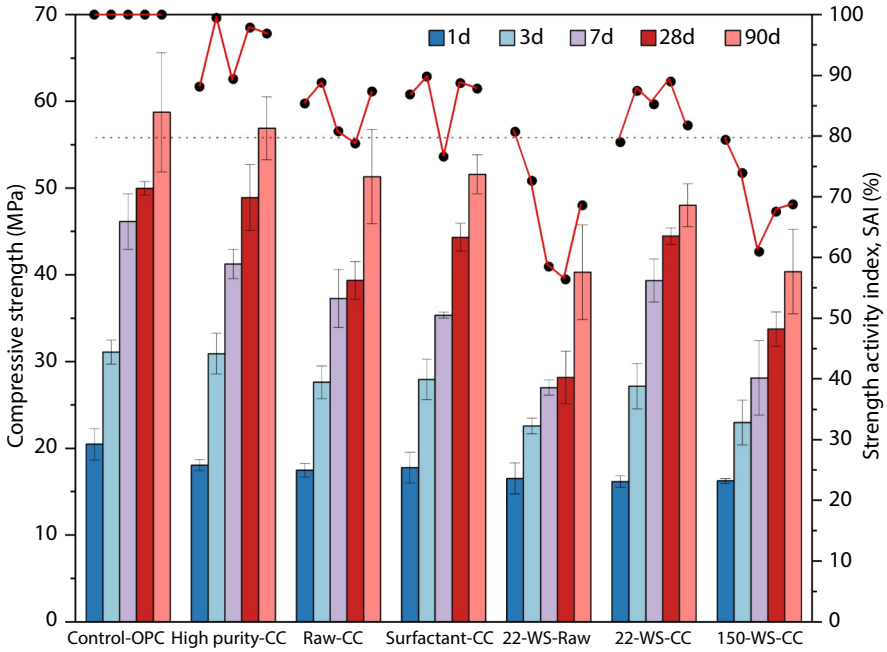

Fig. 10. Compressive strength and strength activity index of each mix.

as to evaluate the effects of clay content. The results derived from this study can be summarized as follows:

1) Quartz removal from marine clay is effectively achieved by the wet sedimentation method, although silt, due to its small particle size, is less efficiently eliminated. Nevertheless, a significant improvement in the mechanical properties of the purified material is observed. It should be noted that under laboratory conditions, the 22 μm sieved wet sedimentation process has reached its limit. Alternative methods, such as vacuum filtration, may be considered in future studies to explore finer sieving effects.

2) Marine clay can be purified by surfactants, with the strength influenced by both effective components of the clay and particle size. Therefore, samples filtered through a 22 μm sieve demonstrate superior strength performance.

3) 22-WS-CC (the 22 μm sieved wet sedimentation process) is recommended by this study. The method utilizes vibration and filtration without the need for any chemical reagents. This approach is more cost-effective and easier to scale up.

Author contribution statement

Qi Luo: Writing – original draft, Methodology, Investigation, Formal analysis, Data curation, Conceptualization. **Xinyu Zhang:** Writing – original draft, Investigation, Formal analysis, Data curation. **Yin Bai:** Investigation, Formal analysis, Data curation. **Guoqing Geng:** Writing – review & editing, Supervision, Project administration, Methodology, Funding acquisition, Formal analysis, Conceptualization.

Declaration of competing interest

Guoqing Geng is an Editorial Board Member for *Materials Reports: Solidwaste and Ecomaterials* and was not involved in the editorial review or the decision to publish this article. The authors declare that they have no known competing financial interests or personal relationships that could have appeared to influence the work reported in this paper.

Acknowledgements

This study was sponsored by the Singapore MOE Tier 2 project (MOE-T2EP50223-0013). Q. Luo acknowledges support by the National Natural Science Foundation of China (Grant 52108269), Natural Science Foundation of Chongqing, China (Grant CSTB2022NSCQ-MSX0347), and China Scholarship Council (CSC, No. 202108500083). X. Zhang acknowledges the Postgraduate Scientific Research Innovation Project of Chongqing Jiaotong University (2024S0001).

References

[1] Luo, Q., Liu, P., Wu, M. Re-using excavated rock from underground tunneling activities to develop eco-friendly ultrahigh performance concrete. *Case Studies in Construction Materials*, **2024**, 20: e02867. https://doi.org/10.1016/j.cscm.2024.e02867.

[2] Luo, Q., Zhang, X., Bai, Y., et al. Reduce the cost and embodied carbon of ultrahigh performance concrete using waste clay. *Case Studies in Construction Materials*, **2023**, 19: e02670. https://doi.org/10.1016/j.cscm.2023.e02670.

[3] Zhang, Z., Yang, F., Liu, J. C., et al. Eco-friendly high strength, high ductility engineered cementitious composites (ECC) with substitution of fly ash by rice husk ash. *Cement and Concrete Research*, **2020**, 137: 106200. https://doi.org/10.1016/j.cemconres.2020.106200.

[4] Scrivener, K., Martirena, F., Bishnoi, S., et al. Calcined clay limestone cements (LC3). *Cement and Concrete Research*, **2018**, 114: 49–56. https://doi.org/10.1016/j.cemconres.2017.08.017.

[5] Avet, F., Snellings, R., Alujas Diaz, A., et al. Development of a new rapid, relevant and reliable (R3) test method to evaluate the pozzolanic reactivity of calcined kaolinitic clays. *Cement and Concrete Research*, **2016**, 85: 1–11. https://doi.org/10.1016/j.cemconres.2016.02.015.

[6] Juenger, M. C. G., Snellings, R., Bernal, S. A. Supplementary ce-

mentitious materials: New sources, characterization, and performance insights. *Cement and Concrete Research*, **2019**, 122: 257–273. https://doi.org/10.1016/j.cemconres.2019.05.008.

[7] Belie, N. D., Soutsos, M., Gruyaert, E. Properties of Fresh and Hardened Concrete Containing Supplementary Cementitious Materials: State-of-the-Art Report of the RILEM Technical Committee 238-SCM, Working Group 4. Berlin: Springer Nature, **2018**: 159. https://doi.org/10.1007/978-3-319-70606-1.

[8] Sánchez Berriel, S., Favier, A., Rosa Domínguez, E., et al. Assessing the environmental and economic potential of limestone calcined clay cement in Cuba. *Journal of Cleaner Production*, **2016**, 124: 361–369. https://doi.org/10.1016/j.jclepro.2016.02.125.

[9] Maraghechi, H., Avet, F., Wong, H., et al. Performance of Limestone Calcined Clay Cement (LC3) with various kaolinite contents with respect to chloride transport. *Materials and Structures*, **2018**, 51(5): 125. https://doi.org/10.1617/s11527-018-1255-3.

[10] Antoni, M., Rossen, J., Martirena, F., et al. Cement substitution by a combination of metakaolin and limestone. *Cement and Concrete Research*, **2012**, 42(12): 1579–1589. https://doi.org/10.1016/j.cemconres.2012.09.006.

[11] He, C., Osbaeck, B., Makovicky, E. Pozzolanic reactions of six principal clay minerals: Activation, reactivity assessments and technological effects. *Cement and Concrete Research*, **1995**, 25(8): 1691–1702. https://doi.org/10.1016/0008-8846(95)00165-4.

[12] Alujas, A., Fernández, R., Quintana, R., et al. Pozzolanic reactivity of low grade kaolinitic clays: Influence of calcination temperature and impact of calcination products on OPC hydration. *Applied Clay Science*, **2015**, 108: 94–101. https://doi.org/10.1016/j.clay.2015.01.028.

[13] Avet, F., Scrivener, K. Investigation of the calcined kaolinite content on the hydration of Limestone Calcined Clay Cement (LC3). *Cement and Concrete Research*, **2018**, 107: 124–135. https://doi.org/10.1016/j.cemconres.2018.02.016.

[14] Kavya Sree, S., Chandra Mohan Rao, B. D. V., Yadav, M. J., et al. Experimental studies on mechanical and durability characteristics of lc_3 concrete. *IOP Conference Series: Materials Science and Engineering*, **2021**, 1091(1): 012075. https://doi.org/10.1088/1757-899x/1091/1/012075.

[15] Sabir, B. B., Wild, S., Bai, J. Metakaolin and calcined clays as pozzolans for concrete: A review. *Cement and Concrete Composites*, **2001**, 23(6): 441–454. https://doi.org/10.1016/S0958-9465(00)00092-5.

[16] Siddique, R., Klaus, J. Influence of metakaolin on the properties of mortar and concrete: A review. *Applied Clay Science*, **2009**, 43(3/4): 392–400. https://doi.org/10.1016/j.clay.2008.11.007.

[17] Heikal, M., El-Didamony, H., Morsy, M. S. Limestone-filled pozzolanic cement. *Cement and Concrete Research*, **2000**, 30(11): 1827–1834. https://doi.org/10.1016/S0008-8846(00)00402-6.

[18] Voglis, N., Kakali, G., Chaniotakis, E., et al. Portland-limestone cements. Their properties and hydration compared to those of other composite cements. *Cement and Concrete Composites*, **2005**, 27(2): 191–196. https://doi.org/10.1016/j.cemconcomp.2004.02.006.

[19] Hartshorn, S. A., Sharp, J. H., Swamy, R. N. Thaumasite formation in Portland-limestone cement pastes. *Cement and Concrete Research*, **1999**, 29(8): 1331–1340. https://doi.org/10.1016/S0008-8846(99)00100-3.

[20] Fernandez, R., Martirena, F., Scrivener, K. L. The origin of the pozzolanic activity of calcined clay minerals: A comparison between kaolinite, illite and montmorillonite. *Cement and Concrete Research*, **2011**, 41(1): 113–122. https://doi.org/10.1016/j.cemconres.2010.09.013.

[21] Badogiannis, E., Kakali, G., Tsivilis, S. Metakaolin as supplementary cementitious material. *Journal of Thermal Analysis and Calorimetry*, **2005**, 81(2): 457–462. https://doi.org/10.1007/s10973-005-0806-3.

[22] Ambroise, J., Murat, M., Péra, J. Hydration reaction and hardening of calcined clays and related minerals V. Extension of the research and general conclusions. *Cement and Concrete Research*, **1985**, 15(2): 261–268. https://doi.org/10.1016/0008-8846(85)90037-7.

[23] Hollanders, S., Adriaens, R., Skibsted, J., et al. Pozzolanic reactivity of pure calcined clays. *Applied Clay Science*, **2016**, 132: 552–560. https://doi.org/10.1016/j.clay.2016.08.003.

[24] Tironi, A., Trezza, M. A., Scian, A. N., et al. Assessment of pozzolanic activity of different calcined clays. *Cement and Concrete Composites*, **2013**, 37: 319–327. https://doi.org/10.1016/j.cemconcomp.2013.01.002.

[25] Beuntner, N., Sposito, R., Thienel, K. C. Potential of calcined mixed layer clays as pozzolans in concrete. *ACI Materials Journal*, **2019**, 116(4). https://doi.org/10.14359/51716677.

[26] Antoni, M. Investigation of cement substitution by blends of calcined clays and limestone. Materials Science, Engineering. **2013**.

[27] Almenares, R. S., Vizcaíno, L. M., Damas, S., et al. Industrial calcination of kaolinitic clays to make reactive pozzolans. *Case Studies in Construction Materials*, **2017**, 6: 225–232. https://doi.org/10.1016/j.cscm.2017.03.005.

[28] Jafari, K., Rajabipour, F. Performance of impure calcined clay as a pozzolan in concrete. *Transportation Research Record: Journal of the Transportation Research Board*, **2021**, 2675(2): 98–107. https://doi.org/10.1177/0361198120953140.

[29] Wang, Q., Yan, Y., Zhang, Z., et al. An LC3-type binder produced with marine clay and municipal waste incineration fly ash. *Construction and Building Materials*, **2024**, 411: 134182. https://doi.org/10.1016/j.conbuildmat.2023.134182.

[30] Jafari, K., Yoon, J., Tokpatayeva, R., et al. Surfactant-assisted purification of an impure kaolinite clay to improve its pozzolanic reactivity in concrete. *Journal of Materials in Civil Engineering*, **2022**, 34(6): 04022094. https://doi.org/10.1061/(asce)mt.1943-5533.0004216.

[31] Gong, S. L., Li, C., Yang, S. L. The microscopic characteristics of Shanghai soft clay and its effect on soil body deformation and land subsidence. *Environmental Geology*, **2009**, 56(6): 1051–1056. https://doi.org/10.1007/s00254-008-1205-4.

[32] Zhu, J. G., Yin, J. H. Strain-rate-dependent stress-strain behavior of overconsolidated Hong Kong marine clay. *Canadian Geotechnical Journal*, **2000**, 37(6): 1272–1282. https://doi.org/10.1139/t00-054.

[33] Ohtsubo, M., Egashira, K., Kashima, K. Depositional and post-depositional geochemistry, and its correlation with the geotechnical properties of marine clays in Ariake Bay, Japan. *Géotechnique*, **1995**, 45(3): 509–523. https://doi.org/10.1680/geot.1995.45.3.509.

[34] Bjerrum, L. Geotechnical properties of Norwegian marine clays. *Géotechnique*, **1954**, 4(2): 49–69. https://doi.org/10.1680/geot.1954.4.2.49.

[35] Bo, M. W., Arulrajah, A., Sukmak, P., et al. Mineralogy and geotechnical properties of Singapore marine clay at Changi. *Soils and Foundations*, **2015**, 55(3): 600–613. https://doi.org/10.1016/j.sandf.2015.04.011.

[36] Sharma, J. S., Chu, J., Zhao, J. Geological and geotechnical features of Singapore: an overview. *Tunnelling and Underground Space Technology*, **1999**, 14(4): 419–31. https://doi.org/10.1016/S0886-7798(00)00005-5.

[37] Hulme, T. W., Burchell, A. J. Tunnelling projects in Singapore: an overview. *Tunnelling and Underground Space Technology*, **1999**, 14(4): 409–18. https://doi.org/10.1016/S0886-7798(00)00004-3.

[38] Chen, Y., Zhao, M., Lv, Y., et al. Utilization of municipal solid waste incineration fly ash as construction materials based on geopolymerization. *Resources, Conservation & Recycling Advances*, **2023**, 19: 200162. https://doi.org/10.1016/j.rcradv.2023.200162.

[39] Sun, D. D., Tay, J. H., Cheong, H. K., et al. Recovery of heavy metals and stabilization of spent hydrotreating catalyst using a glass–ceramic matrix. *Journal of Hazardous Materials*, **2001**, 87(1/2/3): 213–223. https://doi.org/10.1016/S0304-3894(01)00279-5.

[40] Laursen, K., White, T. J., Cresswell, D. J. F., et al. Recycling of an industrial sludge and marine clay as light-weight aggregates. *Journal of Environmental Management*, **2006**, 80(3): 208–213. https://doi.org/10.1016/j.jenvman.2005.08.026.

[41] Hu, Y., Xiong, L., Yan, Y., et al. Performance of limestone calcined clay cement (LC3) incorporating low-grade marine clay. *Case Studies in Construction Materials*, **2024**, 20: e03283. https://doi.org/10.1016/j.cscm.2024.e03283.

[42] Oliver, G., Zaw, K., Hotson, M., et al. U–Pb zircon geochronology of Early Permian to Late Triassic rocks from Singapore and Johor: A plate tectonic reinterpretation. *Gondwana Research*, **2014**, 26(1): 132–143. https://doi.org/10.1016/j.gr.2013.03.019.

[43] ASTM. Standard Test Methods for Sampling and Testing Fly Ash or Natural Pozzolans for Use in Portland-Cement Concrete, **2011**.

[44] Comité Européen de Normalisation. Methods of testing cement - Part 1: Determination of strength. EN 196-1, **2016**.

[45] Wang, Y., Ramanathan, S., Burris, L., et al. A rapid furnace-based gravimetry test for assessing reactivity of supplementary cementitious materials. *Materials and Structures*, **2022**, 55(7): 193. https://doi.org/10.1617/s11527-022-02029-0.

[46] State Administration for Market Regulation, Standardization Administration of the People's Republic of China. Test method of cement mortar strength (ISO method). GB/T 17671-2021, **2021**.

[47] Chew, S. H., Kamruzzaman, A. H. M., Lee, F. H. Physicochemical and engineering behavior of cement treated clays. *Journal of Geotechnical and Geoenvironmental Engineering*, **2004**, 130(7): 696–706. https://doi.org/10.1061/(asce)1090-0241(2004)130:7(696).

[48] Sun, D. D., Tay, J. H., Easton, C. Recovery and encapsulation of heavy metals on refinery spent hydrotreating catalyst. *Water Science and Technology*, **2000**, 42(5/6): 71–77. https://doi.org/10.2166/wst.2000.0497.

[49] Du, H., Pang, S. D. Value-added utilization of marine clay as cement replacement for sustainable concrete production. *Journal of Cleaner Production*, **2018**, 198: 867–873. https://doi.org/10.1016/j.jclepro.2018.07.068.

[50] Leo, E. S., Alexander, M. G., Beushausen, H. Optimisation of mix proportions of LC3 binders with African clays, based on compressive strength of mortars, and associated hydration aspects. *Cement and Concrete Research*, **2023**, 173: 107255. https://doi.org/10.1016/j.cemconres.2023.107255.

[51] Ungár, T. Microstructural parameters from X-ray diffraction peak broadening. *Scripta Materialia*, **2004**, 51(8): 777–781. https://doi.org/10.1016/j.scriptamat.2004.05.007.

[52] Scrivener, K. L., Juilland, P., Monteiro, P. J. M. Advances in understanding hydration of Portland cement. *Cement and Concrete Research*, **2015**, 78: 38–56. https://doi.org/10.1016/j.cemconres.2015.05.025.

[53] Frías, M., Cabrera, J. Influence of MK on the reaction kinetics in MK/lime and MK-blended cement systems at 20 °C. *Cement and Concrete Research*, **2001**, 31(4): 519–527. https://doi.org/10.1016/S0008-8846(00)00465-8.

[54] Hesse, C., Goetz-Neunhoeffer, F., Neubauer, J. A new approach in quantitative *in situ* XRD of cement pastes: Correlation of heat flow curves with early hydration reactions. *Cement and Concrete Research*, **2011**, 41(1): 123–128. https://doi.org/10.1016/j.cemconres.2010.09.014.

[55] Zhang, X., Bai, Y., Luo, Q. Exploring synergistic effects and hydration mechanisms in metakaolin-blended cement system with varying metakaolin and wollastonite content. *Construction and Building Materials*, **2024**, 425: 135962. https://doi.org/10.1016/j.conbuildmat.2024.135962.

[56] Jain, J., Neithalath, N. Analysis of calcium leaching behavior of plain and modified cement pastes in pure water. *Cement and Concrete Composites*, **2009**, 31(3): 176–185. https://doi.org/10.1016/j.cemconcomp.2009.01.003.

[57] Scrivener, K, Snellings, R, Lothenbach, B. A Practical Guide to Microstructural Analysis of Cementitious Materials. Boca Raton: CRC Press, **2015**:198. https://doi.org/10.1201/b19074.

[58] Bernal, I. M. R., Shirani, S., Cuesta, A., et al. Phase and microstructure evolutions in LC3 binders by multi-technique approach including synchrotron microtomography. *Construction and Building Materials*, **2021**, 300: 124054. https://doi.org/10.1016/j.conbuildmat.2021.124054.

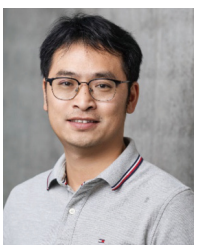

Qi Luo, an Independent Principal Investigator at Aarhus University and a Humboldt Fellow at RWTH Aachen University. Before joining Aarhus University, he held research positions at Chongqing Jiaotong University (China) and the National University of Singapore. His research focuses on the sustainability and durability of cementitious materials, particularly in multi-scale damage mechanics, mechanical performance, life cycle assessment (LCA), and the development of multifunctional cement-based materials. His work has been supported by prestigious funding agencies, including the Villum Foundation, the Humboldt Foundation, and the National Natural Science Foundation of China, among others.

Guoqing Geng received his doctoral degree from the University of California at Berkeley in 2017. His PhD program was dedicated to investigating the microscale chemistry and mineralogy of modern construction materials. He was then awarded a postdoctoral fellowship at the Paul Scherrer Institute (Switzerland), where he studied the durability of concrete both as a construction material and hosting material for radioactive waste. He joined the Department of Civil and Environmental Engineering at the National University of Singapore in 2019. He has research interests in sustainability and performance-based designing of modern construction materials, as well as predicting and enhancing their long-term durability.